European Conf. on Computer Vision (ECCV)
Workshop for Vision on Cognitive Tasks, 2010.

Matching and Predicting Street Level Images

Biliana Kaneva[1], Josef Sivic[2], Antonio Torralba[1], Shai Avidan[3], and William T. Freeman[1]

[1]Massachusetts Institute of Technology
{biliana,torralba,billf}@csail.mit.edu
[2] INRIA, WILLOW, Laboratoire d'Informatique de l'Ecole Normale Superieure
Josef.Sivic@ens.fr
[3]Tel-Aviv University, Adobe Research
shai.avidan@gmail.com

Abstract. The paradigm of matching images to a very large dataset has been used for numerous vision tasks and is a powerful one. If the image dataset is large enough, one can expect to find good matches of almost any image to the database, allowing label transfer [3, 15], and image editing or enhancement [6, 11]. Users of this approach will want to know how many images are required, and what features to use for finding semantic relevant matches. Furthermore, for navigation tasks or to exploit context, users will want to know the predictive quality of the dataset: can we predict the image that would be seen under changes in camera position?
We address these questions in detail for one category of images: street level views. We have a dataset of images taken from an enumeration of positions and viewpoints within Pittsburgh. We evaluate how well we can match those images, using images from non-Pittsburgh cities, and how well we can predict the images that would be seen under changes in camera position. We compare performance for these tasks for eight different feature sets, finding a feature set that outperforms the others (HOG). A combination of all the features performs better in the prediction task than any individual feature. We used Amazon Mechanical Turk workers to rank the matches and predictions of different algorithm conditions by comparing each one to the selection of a random image. This approach can evaluate the efficacy of different feature sets and parameter settings for the matching paradigm with other image categories.

1 Introduction

An important resource for the computer vision research community is the many images available through the Internet or large-scale acquisition and storage. A natural task for a large dataset, not possible for smaller ones, is to find close visual matches to a test image. While each image is unique, in a large dataset, close enough matches may be found to enable transfer of the object or region labels the retrieved image may have [3, 15], or exploiting the retrieved images for editing [11] or enhancement [6] of the query image.

We call the task of finding a semantically meaningful matches to a test image the *matching* task. To make the matching task feasible in the applications

above, the set of retrieved images is usually restricted to some category, such as indoor scenes, faces, or city images taken from street level. To support this class of computer vision algorithm, we need to understand various fundamental properties of this approach. How well do the methods scale with the dataset size? What are the best features to use to find semantically meaningful nearest neighbor matches?

The matching task asks how well a collection of test images can match a dataset of images, and indicates the coverage of a set of test images by the reference database. To study the structure of all the images within the given category, we also want to address the *prediction* task: how well can images from one camera position and orientation predict the image taken by a camera at a neighboring position or orientation? This tells us spatial regularities within the image database, and has applications in two broad domains: to study spatial consistencies within the image database, and to predict images from a moving camera. Knowledge of such regularities is needed to form more powerful image prior probabilities, useful for image synthesis and reconstruction (for example, [6, 9]). The prediction task provides another way to ask a question of importance in the object recognition community, how well can context predict image content [7, 24]? The prediction task is used implicitly by mobile agents in the world (people or robots) in deciding where to look or move next.

We want to know: how well can we match? how well can we predict? what are the regularities of the visual world, and how accessible are they through large datasets? We will study this problem restricted to one class of images: outdoor street scenes. The restriction to one image category provides us with a variety of images, yet a tractable set. This class of images is of commercial interest for mapping and commerce.

There have been informal studies of matching or prediction for individual applications [11, 21], but systematic study of these properties have not been undertaken. In the past, large image databases were used to fill in holes in an image [11] or create infinite images from photographs taken at the different locations in the real world [21]. The evaluation of [11] did not address the tasks of matching or prediction, and the method was user-assisted, not automatic as ours is. Prior work on multiperspective panoramas [1, 19, 27] focuses on using large number of images all taken from the same location but from different view points and stitching them together. Similarly, the PhotoTourism interface [22] places a large collection of images of one particular geographic location in a common 3D space. Here we use image transformations similar to those of [21] but we focus on a database of outdoor city scenes from many different parts of the world that were downloaded from various photo sharing websites. In addition, we design and execute an quantitative experimental evaluation and compare several state-of-the-art image descriptors for the matching and prediction tasks.

To measure how well the system works, we use a ground truth database synthesized from 10,000 geo-referenced images from the Google Street View data set of Pittsburgh [10].

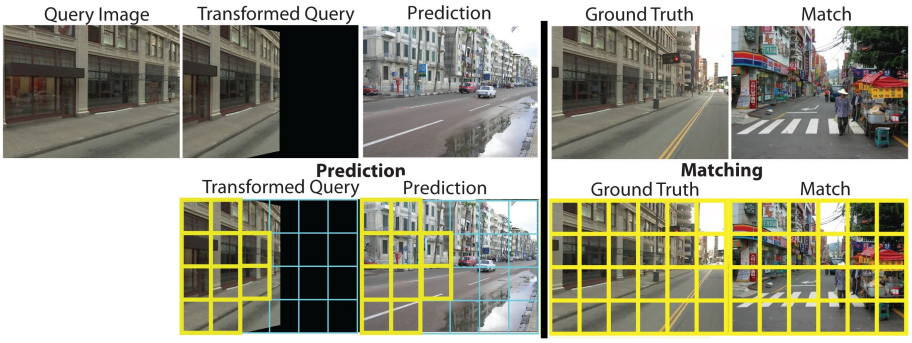

Fig. 1. Prediction and matching. Top row: Query Image. Transformed query image for rotate right motion. The prediction obtained by finding the nearest neighbor using the transformed query (the prediction task). Ground truth (the actual view seen after the camera rotated from the query image). Top match to the ground truth image (the matching task). Bottom row: The transformed query image and the top prediction image retrieved with the bins used for retrieval overlaid. The ground truth and the top match images and the bins used for the retrieval overlaid.

In the matching task, we ask how well can we explain street-level images from Pittsburgh from outdoor images taken in any city other than Pittsburgh? In the prediction task, we ask what regularities are in common across images of Pittsburgh and of other cities in the world such that we can predict images of Pittsburgh under different camera transformations? The matching and prediction tasks are illustrated in figure 1. We conduct large scale experiments to evaluate both the matching task and the prediction task using various image representation methods, various database size and various camera motions (for prediction). We evaluate the quality of the matches and predictions in a user study performed using Amazons Mechanical Turk web service.

2 Database, Features, and Transformations

In this section we describe our image database, give details of the compared image features, and outline our image matching and prediction methods.

2.1 Image database

Our premise is that if we had enough images of the world, we will be able to make predictions about what is around us. Here, we focus on images of an urban environment. We created a large database of 100,000 images of outdoor street scenes downloaded from Flickr. The images typically have resolution of 500x375 pixels. We used image tag information, e.g. "Paris street" or "Seattle alley", to select candidate city street scenes. Due to noise in the tags, there were many images that did not belong to the outdoor city theme, including indoor scenes and portraits of people. To reduce the amount of noise, we trained an SVM scene classifier, similar to [4, 14], to prune out the images that do not

belong to the city theme. We manually labeled the training data of 1000 positive and 2000 negative training images with the help of a labeling interface that we have developed. The tool allows the user to interactively train the classifier and provides visual feedback about its performance after each iteration. It can be used for the creation of databases with other themes. Currently, we only consider images in landscape format with aspect ratio close to 4:3.

2.2 Image representations

Here we describe the different image representations we investigate for the matching and prediction tasks. Similar representations were used by [28] for the tasks of scene detection and classification.

i. GIST descriptor: The GIST descriptor has been shown to work well for scene classification [18]. It measures the oriented edge energy at different scale levels aggregated into coarse spatial bins. We create a 480 dimensional feature vector by first converting the image to grayscale and then dividing it in 6x4 bins and applying 8, 8, and 4 orientation filters at three difference scales (coarse to fine) to each bin. The GIST descriptor for each image is normalized to have unit L2 norm.

ii. Histograms of oriented gradients (HOG): The HOG descriptor [5] and its variants [8] have demonstrated excellent performance for object and human detection. Similar to the SIFT [16], the HOG descriptor measures histograms of image gradient orientation at a coarse grid of spatial locations. First, HOG descriptors are densely extracted on a regular grid at steps of 8 pixels using the code available online provided by [8]. This gives a 31-dimension descriptor for each node of the grid. Then, 2x2 neighboring HOG descriptors are stacked together to form a descriptor with 124 dimensions. The stacking has overlapping on the grid, and the 124-dimension descriptors are quantized into 300 visual words by k-means. The quantized descriptors are then spatially binned into a coarse grid of 6x4 bins, similar to the GIST descriptor. The resulting histogram is normalized to have unit L1 norm.

iii. The self-similarity descriptor (SSIM): The self-similarity descriptor [20] has been shown to perform well on matching objects of similar shape but vastly different local appearance. The idea is to represent the appearance in a local image area around a particular image patch by the "correlation map" of the patch with its neighborhood. The descriptor captures the local pattern of self-similaritiy. Such self-similarity patterns can then be matched despite a very different appearance of the central patch. We employ the self-similarity descriptor for scene representation.

The self-similarity descriptors are computed on a regular grid at steps of five pixels. Each descriptor is obtained by computing the correlation map of a 5x5 patch in a window with radius equal to 40 pixels, then quantizing it in 3 radial bins and 10 angular bins, obtaining 30 dimensional descriptor vectors. The descriptors are then quantized into 300 visual words by k-means. Similar to HOG, the self-similarity descriptors are spatially binned into a coarse grid of 6x4 bins, and normalized to have unit L1 norm.

iv. Dense SIFT: Densely extracted SIFT descriptors have been shown to work well in both object and scene recognition [14]. Here, we extract the descriptor on a regular grid at steps of 5 pixels using a window at two scales (4x4 and 8x8). The descriptors are stacked together for each HSV color channel and quantized into 300 visual words by k-means. The quantized descriptors are then spatially binned into a coarse grid of 6x4 bins, similar to the GIST descriptor. The resulting histogram is normalized to have unit L1 norm.

v. Geometric context (GC): The geometric context classifiers [12] estimate the coarse geometric layout of natural scenes with respect to the camera. It has been shown to work well as a spatial prior for object detectors [13]. Here we investigate it for the task of scene matching and prediction. We use only the (i) ground, (ii) sky, (iii) vertical and (iv) porous classes as they are more reliably detected. We reduce the probability outputs of each of the four geometric classes to 32x32 pixels resulting in a 256-dimensional descriptor. The resulting descriptor is normalized to have unit L2 norm.

vi. Tiny images (Tiny32): As a baseline we also include the tiny image representation of Torralba *et al.* [25]. The most trivial way to match scenes is to compare them directly in color image space. Reducing drastically the image dimensions makes this approach more computationally feasible and less sensitive to exact alignment. This method of image matching has been examined thoroughly [25] for the purpose of object recognition and scene classification. Each of the RGB channels is subsampled to 32x32 pixels resulting in a 3,072 dimensional descriptor. The images are then normalized to have unit L2 norm.

vii. Texton histogram: Textons as elementary units in image analysis were introduced in [17]. We use a 512 entry universal texton dictionary built by clustering the responses of filters at 8 different orientations, 2 different scales and elongations. We then build a 512-dimensional histograms spatially binned into a coarse grid of 6x4 bins by assigning the result of the filter responses at each pixel to the nearest texton dictionary entry. The histogram is normalized to have unit L1 norm.

viii. Color histogram: We compute color histograms in CIE L*a*b* color space with 4, 14, and 14 bins in L, a, and b, similar to [28]. The histograms are then spatially binned into a coarse grid of 6x4 bins and normalized to unit L1 norm.

Next we describe the matching and description procedures.

2.3 Nearest neighbor image matching

In the matching task, the goal is to find the best matching image in the street scene database given the query. Recently, there has been some success in semantic scene matching using nearest neighbor techniques in large databases of millions of images [11, 25] and we follow this work here. This matching is performed using an exhaustive nearest neighbor search, though faster but approximate

indexing techniques could be used [26]. For the (normalized) GIST, tiny image and geometric context descriptors we use the Euclidean distance. For the HOG, self-similarity, dense SIFT, texton and color histograms we use the χ^2 distance.

We also investigate a combination of all descriptors (denoted All). This is achieved by a simple weighted average of the distances using individual descriptors. Here we investigate uniformly set weights, but weights learnt on a separate training set can be also used [2]. Uniform weights are a reasonable choice in our case, as the range of distances for each of the normalized descriptors is between 0 and 1.

2.4 Prediction using transformed image retrieval

In the prediction task, we would like to predict what we will see if we move the camera. Given a query image, we want to find possible candidates describing the parts of the scene not captured by the camera. We extend traditional image retrieval to find matches that simulate a particular camera motion without explicitly modeling the geometry of the scene. Instead, we apply 2D transformations to the query image. We achieve horizontal camera rotation by warping the image using the appropriate homography [23](page 11)

$$\mathtt{H} = \mathtt{K}\mathtt{R}\mathtt{K}^{-1}, \tag{1}$$

where $\mathtt{K}$ is the internal calibration matrix and $\mathtt{R}$ the camera rotation matrix. For specifying $\mathtt{K}$, we set the unknown focal length to be half the image width. For specifying $\mathtt{R}$ we assume no vertical or in-plane rotation. The 3D zoom-out motion (or backward motion) is approximated by scaling the image ignoring the parallax effects. The transformed query image has missing pixels because not all the information of what the camera would see after the transformation is available in the original query image. Therefore, we can only use a subset of the feature vector to perform the transformed image retrieval (Fig. 1). Given the observed portion of the transformed query image, we can now find semantically similar images that approximate the new camera point of view. For rotation, we take about half of the overlapping image. For zoom, we use a scaled version of the image depending on the amount of zoom. The retrieval is performed using the nearest neighbor search as outlined in section 2.3 but only using the observed portion of the transformed query image.

3 Evaluation methods

To compare the different descriptors for the matching and prediction tasks we have collected the following ground truth image test set and designed an evaluation procedure based on human judgment of visual similarity.

3.1 Ground truth data set

We gathered ground truth data from the Google Street View Pittsburgh data set [10], which is provided by Google for research purposes. The data set contains about $10,000$ high-resolution spherical panoramas collected by a moving vehicle

for the Street View feature of Google Maps. Each panorama has a field of view of 360 degrees horizontally and 180 degrees vertically. To synthesize images similar to those in our Flickr city database, we unwarp portions of the spherical panoramas simulating a camera with 45 degree field of view with rotation stops at every 22.5 degrees [23]. From the synthesized images, we selected 300 representative pairs for each motion - rotate right, and zoom out - for our ground truth data set. Each pair contains the query image for our test set and its corresponding ground truth match based on the camera motion. Having ground truth data allows us to measure the quality of the different image representations used for matching and making predictions about what the camera would see if it performed a given camera motion.

3.2 Performance measures

As a performance measure we use human judgment of visual similarity of the matched / predicted image to the ground truth. We sought to evaluate the visual quality of the images retrieved using a variety of different feature descriptors. Rather than assessing pairwise comparisons between each possible descriptor's results, we compared the results from each feature descriptor against a random selection from the image database. This allowed us to evaluate performance of all the descriptors with respect to a common scale and reduced the complexity of the evaluation task.

We designed and conducted experiments using the Amazon Mechanical Turk to compare the performance of the different features for the matching and prediction tasks. We divided each experiment of 300 test query images into 10 tasks and each task contained 30 examples.

To evaluate the prediction performance, an example included (i) the ground truth image G (the actual view after the camera transformation), (ii) the predicted image P from the database obtained using the transformed image retrieval and (iii) a random image R from the database (Fig. 2). The users were then asked to select which one of the (ii) predicted image or the (iii) random image was most like the (i) ground truth image, based on visual similarity of the scene type, common objects and their locations in the images. The predicted and random images were presented in a random order to eliminate possible bias if users had a preference in selecting the first or the second image more often. The random image in the triplet is kept the same across different evaluated features. The chance performance for this task is 50%. The best performance, i.e. if the users prefer the predicted image over the random image for all 300 test queries, would be 100%

Similarly, to evaluate the matching task an example included: (i) the ground truth image G, (ii) the best match from the database B (obtained by matching directly on G without a transformation), and (iii) a random image R from the database.

To ensure the quality of the work, we set a qualification requirement that allowed only users with 95% task acceptance rate to participate. Furthermore, we added six control examples to each task presented in a random order. The control examples had a clear correct answer and allowed us to remove users that

Fig. 2. Single example from the user study showing the ground truth G, prediction P and random R images presented to the user. Comparison to the random guess allows for evaluation and ranking of the different image representations (feature sets) relative to each other.

were not paying attention throughout the entire task. Tasks with less than 100% correct responses to the control examples were discarded, approximately 10-15% of the data. Each task was completed by 10 different users.

We performed a number of experiments using test examples generated from different descriptors and different database sizes. Over 100 different users participated in the user study. For each example, we had between 8 and 10 votes for the image that best predicted the ground truth image. The results for each experiment were evaluated by the majority vote. If more than 50% of the users selected the predicted image as the image that explained best the ground truth image, then we say the users preferred the predicted image. Note that the random images are kept the same across different users.

4 Experiments

We use the ground truth data to evaluate (i) the matching performance and (ii) the prediction performance for each camera motion. To evaluate prediction, we use the transformed query Q to find the best match P that should predict the ground truth image G that the camera would see after performing a particular motion. To evaluate matching, we use the ground truth image G to find the best match B in the database. We consider the following two motions - rotate right by 22.5 degrees, and 2x zoom out. Performance is measured on the ground truth dataset of 300 queries by the user preference rate vs. the random image as outlined in section 3.

We compared the performance for both the matching and prediction tasks using the different feature descriptors as well as a combination of all the descriptors. Results are summarized in figure 3 and exact user preference rates are given in table 1. Examples of the best matches and predictions for the rotate right and zoom-out motions are shown in figure 6 (a) and (b), respectively. Figure 5 shows examples of good and poor predictions for the HOG descriptor, compared to the random image, as judged by the Mechanical Turk workers.

Comparison of different scene descriptors: The best prediction performance is achieved by a combination of all of the descriptors as shown in Fig. 3. The clear winner among the individual descriptors in both the prediction and the matching tasks is the HOG feature descriptor as shown in Fig. 3. It performs extremely well for the zoom out motion with 92% preference rate in the matching task and 84% in the prediction task. This is interesting and confirms the good performance of bag-of-features methods with coarse spatial binning for image and scene classification tasks [14, 4] (though these methods are based on the quantized SIFT [16] descriptor rather than quantized HOG [5]). The prediction results using the dense SIFT descriptor are similar to those of the HOG descriptor for both types of motions, however the HOG descriptor performs better in the matching task. For the rotate right motion, the geometric context (GC), self-similarity descriptor (SSIM), GIST and the color and texton histograms perform about the same – around 60%. The tiny image descriptor performs slightly above the chance performance (50%).

Matching vs. prediction performance: In the majority of the cases, the descriptors performed better at the matching task. This is to be expected since there is more information available in this case as we use the entire ground truth image to retrieve similar images from the database. For prediction, only the visible portion of the transformed query image is used (Fig. 1). Nevertheless, the significantly above chance (50%) results on the prediction task (77% for rotate-right and 88% for zoom-out) suggest it is possible, to some extent, to predict the appearance outside the boundary of the image for the street scenes considered in this work.

Interestingly, the performance of the self-similarity descriptor (SSIM) in the prediction task is significantly better than that for the matching task. One possible explanation are the matches on night images (see the fourth column of the top row of Fig. 6 (b) for the SSIM descriptor). The self-similarity descriptor is largely invariant to illumination. The users were generally influenced by color when selecting similar images even though they were not explicitly asked to compare the images based on color appearance.

For zoom-out motion, the geometric context (GC) is performing significantly worse for prediction than matching. This might be due to the fact that for the zoom-out prediction the transformed retrieval uses only the middle portion of the database images. This typically excludes the ground plane region – an important feature for geometric context.

Rotate vs. zoom-out motion: Most of the descriptors perform better in the matching task for the zoom out motion than for the rotate right motion, despite the fact that the matching task is the same for both motions (i.e. no transformation is applied to the query). This is likely due to the nature of our ground truth test datasets where most of the images for the zoom out motion are perspective views of streets (see Fig. 6 (b)), which are well represented in the database of Flickr images. For the rotate motion the test set is more varied making the task considerably harder. Similar behavior is observed for the prediction task, further emphasizing the easier nature of the zoom-out motion test data.

Motion	Rotate Right		Zoom Out	
Features	Matching	Prediction	Matching	Prediction
All	**80%**	**77%**	**86%**	**88%**
HOG	**78%**	**69%**	**92%**	**84%**
Dense SIFT	69%	69%	85%	84%
GC	64%	61%	71%	40%
Color Hist	63%	63%	57%	61%
Texton Hist	63%	61%	89%	85%
SSIM	62%	54%	77%	85%
GIST	59%	61%	64%	63%
Tiny32	56%	55%	74%	73%

Table 1. Performance of the different features in the matching and prediction tasks (sorted by performance).

The effect of increasing database size: We performed an additional experiment varying the size of the database of Flickr images between 1K, 10K, and 100K. For this experiment, we used the best performing feature descriptor on the 100K database (HOG) with the rotate right and zoom out motions. We selected a random subset of 1K and 10K images from our 100K database. The matching and prediction performance is shown in figure 4. Increasing the database size from 1K to 10K results in a marked improvement for both the matching and prediction tasks for the rotate right motion (Fig. 4 (a)). However, the performance does not change significantly as the database increases to 100K images. In fact, the prediction performance decreases slightly for the 100K dataset, though this decrease is likely to be within the evaluation error (due to the random selection of comparison images). The performance for the zoom out motion for both tasks does not change significantly with the change in database size. Others have observed a steady increase in image matching performance with database size for recognition [25] or computer graphics [11] applications. In our case, the lack of observable improvement for the zoom out motion and when going from the 10K to the 100K dataset for the rotate right motion might be due to the fact that our Flickr database has been carefully pre-filtered (section 2) to contain mostly street scenes. The use of a scene classifier to select the images in our dataset may have reduced the variability in the data where adding images beyond 1K (for zoom out) or 10K (for rotate right) does not provide any additional information to make the tasks easier to solve. The reason for the lower bound for zoom out motion may be due to the easier nature of the ground truth data set where most of the scenes are of perspective street views.

5 Conclusions

We have studied the properties of an instance of a general computer vision algorithm: match a test image to examples in a large dataset of images of the corresponding class (street level views, in this case). This general approach has many current and potential applications [15, 3, 11, 6], and we study fundamental issues: How many images do we need to find semantically meaningful matches?

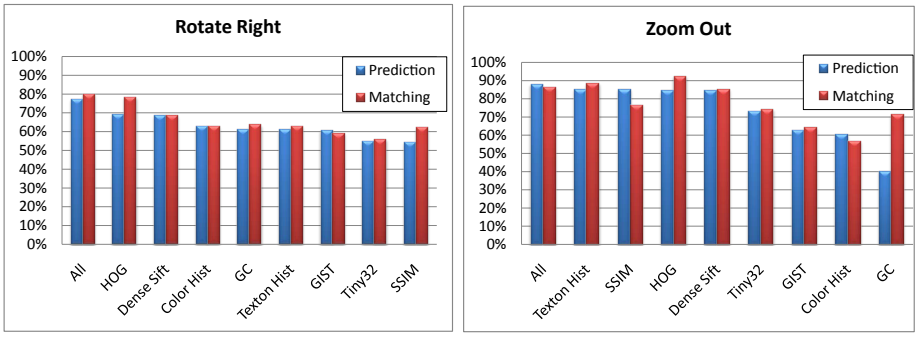

(a) (b)

Fig. 3. Performance of the different features in the matching and prediction tasks (sorted by matching performance). a) Rotate Right. b) Zoom Out.

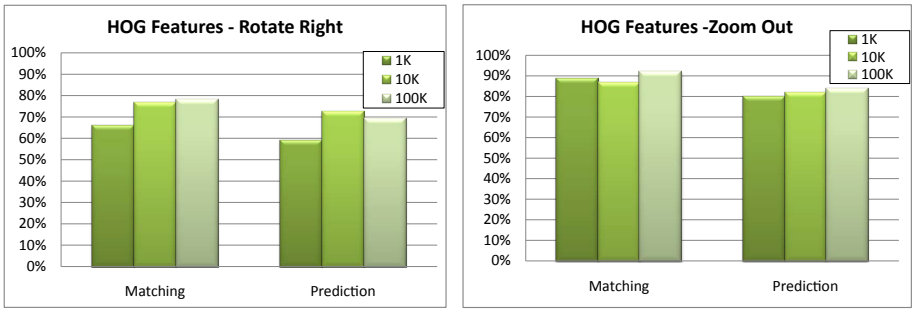

(a) (b)

Fig. 4. Performance of HOG feature descriptor on different database sizes. a) Rotate Right. b) Zoom Out.

What features should we use to do so? Further, we study properties of the images in the class with respect to navigation, and we ask: how regular is the image dataset across changes in camera position?

We use Amazon Mechanical Turk workers to judge image matching and prediction performance relative to a random image choice as a way to assess the relative power of different algorithm choices.

We find that histograms of quantized HOG features worked best of the eight individual categories of features we tested. A dataset size of 100,000 images was sufficient to match images with 78 to 92 percent favoring the retrieved image over a random selection. We found there was sufficient regularity in the streetview datasets to predict images at new camera positions, almost to the accuracy to which images can be matched. In this case, a combination of all the features performed better than any individual feature set alone. The experiments described here allow us to calibrate and characterize datasets for the matching and prediction tasks, useful for dataset driven recognition and navigation.

Fig. 5. Examples of image triplets shown to the user. The first three columns show examples where the users picked the prediction based on the HOG feature descriptor from a 100K database. The second three columns show examples where the users preferred the random image.

Acknowledgements

We acknowledge the funding support of ARDA VACE, NGA NEGI-1582-04-0004, MURI Grant N00014-06-1-0734, ANR project HFIBMR (ANR-07-BLAN-0331-01), the MSR-INRIA laboratory and a Xerox Fellowship.

References

1. A. Agarwala, M. Agrawala, M. Cohen, D. Salesin, and R. Szeliski. Photographing long scenes with multi-viewpoint panoramas. *ACM Transactions on Graphics*, 2006.
2. F. R. Bach, R. Thibaux, and M. I. Jordan. Computing regularization paths for learning multiple kernels. In *Advances in Neural Information Processing Systems*, 2004.
3. A. C. Berg, T. L. Berg, and J. Malik. Shape matching and object recognition using low distortion correspondence. In *IEEE Computer Vision and Pattern Recognition (CVPR)*, 2005.
4. A. Bosch, A. Zisserman, and X. Munoz. Scene classification using a hybrid generative/discriminative approach. *IEEE Trans. Pattern Analysis and Machine Intelligence*, 30(4), 2008.
5. N. Dalal and B. Triggs. Histograms of oriented gradients for human detection. In *Proc. IEEE Conf. Computer Vision and Pattern Recognition*, 2005.
6. K. Dale, M. K. Johnson, K. Sunkavalli, W. Matusik, and H. Pfister. Image restoration using online photo collections. In *IEEE International Conference on Computer Vision (ICCV)*, 2009.

7. S. Divvala, D. Hoiem, J. Hays, A. Efros, and M. Hebert. An empirical study of context in object detection. In *Proceedings of the IEEE Conf. on Computer Vision and Pattern Recognition (CVPR)*, June 2009.
8. P. Felzenszwalb, D. McAllester, and D. Ramanan. A discriminatively trained, multiscale, deformable part model. In *Proc. IEEE Conf. Computer Vision and Pattern Recognition*, 2008.
9. R. Fergus, B. Singh, A. Hertzmann, S. T. Roweis, and W. Freeman. Removing camera shake from a single photograph. *ACM Transactions on Graphics, SIGGRAPH 2006 Conference Proceedings, Boston, MA*, 25:787–794, 2006.
10. Google. Google Street View Pittsburgh data set. In *http://maps.google.com/help/maps/streetview/*, 2008.
11. J. Hays and A. A. Efros. Scene completion using millions of photographs. *Proc. ACM SIGGRAPH*, 26(3):4:1–4:7, 2007.
12. D. Hoiem, A. Efros, and M. Hebert. Geometric context from a single image. In *Proc. IEEE Int. Conf. Computer Vision*, 2005.
13. D. Hoiem, A. Efros, and M. Hebert. Putting objects in perspective. In *Proc. IEEE Conf. Computer Vision and Pattern Recognition*, 2006.
14. S. Lazebnik, C. Schmid, and J. Ponce. Beyond bags of features: Spatial pyramid matching for recognizing natural scene categories. In *Proc. IEEE Conf. Computer Vision and Pattern Recognition*, 2006.
15. C. Liu, J. Yuen, and A. Torralba. Dense scene alignment using SIFT flow for object recognition. In *Proc. IEEE Conf. Computer Vision and Pattern Recognition*, 2009.
16. D. Lowe. Object recognition from local scale-invariant features. In *Proc. IEEE Int. Conf. Computer Vision*, Sept. 1999.
17. J. Malik, S. Belongie, J. Shi, and T. Leung. Textons, contours and regions: Cue integration in image segmentation. In *Proc. IEEE Int. Conf. Computer Vision*, pages 918–925, 1999.
18. A. Oliva and A. Torralba. Modeling the shape of the scene: a holistic representation of the spatial envelope. *Int. Journal of Computer Vision*, 42(3):145–175, 2001.
19. P. Rademacher and G. Bishop. Multiple-center-of-projection images. *ACM Transactions on Graphics*, 1998.
20. E. Shechtman and M. Irani. Matching local self-similarities across images and videos. In *Proc. IEEE Conf. Computer Vision and Pattern Recognition*, 2007.
21. J. Sivic, B. Kaneva, A. Torralba, S. Avidan, and W. T. Freeman. Creating and exploring a large photorealistic virtual space. In *First IEEE Workshop on Internet Vision*, 2008.
22. N. Snavely, S. M. Seitz, and R. Szeliski. Photo tourism: Exploring photo collections in 3D. In *Proc. ACM SIGGRAPH*, 2006.
23. R. Szeliski. Image alignment and stitching: A tutorial. *Foundations and Trends in Computer Graphics and Computer Vision*, 2006.
24. A. Torralba. Contextual priming for object detection. *Int. Journal of Computer Vision*, 53:169–191, 2003.
25. A. Torralba, R. Fergus, and W. T. Freeman. 80 million tiny images: a large dataset for non-parametric object and scene recognition. *IEEE Trans. Pattern Analysis and Machine Intelligence*, 30(11):1958–1970, 2008.
26. Y. Weiss, A. Torralba, and R. Fergus. Spectral hashing. In *Advances in Neural Information Processing Systems*, 2009.
27. D. N. Wood, A. Finkelstein, J. F. Hughes, C. E. Thayer, and D. Salesin. Multiperspective panoramas for cel animation. *ACM Transactions on Graphics*, 1997.
28. J. Xiao, J. Hays, K. A. Ehinger, A. Torralba, and A. Oliva. SUN database: Large scale scene recognition from Abbey to Zoo. In *Proc. IEEE Conf. Computer Vision and Pattern Recognition*, 2010.

Fig. 6. Example matches and predictions on a 100K database. a) Rotate Right. b) Zoom Out. For each descriptor the images shown in: Top row - Matches to the ground truth; Bottom row - Predictions of the ground truth image based on the query image.